ELSEVIER

Catalysis Today 50 (1999) 579–588

CATALYSIS TODAY

On the mechanism and energetics of Boudouard reaction at FeO(1 0 0) surface: $2CO \rightarrow C + CO_2$

Hansong Cheng*, David B. Reiser, Sheldon Dean Jr.

Air Products and Chemicals, Inc., Research and Engineering Systems, 7201 Hamilton Boulevard, Allentown, PA 18195-1501, USA

Abstract

We present a density functional study on the mechanism of metal dusting at surfaces of transition metal oxides. The present study focuses on one of the major metal dusting processes: the Boudouard reaction on FeO(1 0 0) surface. Cluster models are used to represent the surface and the effects of cluster sizes and relaxation upon CO adsorption are carefully examined. It is found that the CO adsorption on a well-aligned transition metal oxide surface is very weak and does not lead to CO-bond dissociation. A minimum energy path of a gas-phase CO attacking an adsorbed CO from the surface normal is calculated and the structural change of the reaction species along the reaction path is examined. The results suggest that the Boudouard reaction is extremely unfavorable energetically at the transition metal oxide surfaces and that a pitting mechanism dictates the dusting process, in agreement with practical observations.

Keywords: Transition metal oxides; Boudouard reaction; Metal dusting process

1. Introduction

Metal dusting is a catastrophic corrosion processes that frequently occurs in many industrial processes such as synthesis gas production, coal gasification and iron ore reduction [1–6]. The dominant chemical processes include the chemisorption of carbon monoxide at alloy or stainless steel surfaces and the subsequent deposition of carbon on these materials resulting from the interaction between the adsorbed species and the gas steams through the Boudouard and steam–carbon reactions at high temperature [3–6]. The two reactions are, respectively, described by the following processes:

$$CO + CO \rightarrow C + CO_2$$

$$CO + H_2 \rightarrow C + H_2O$$

As a consequence of dusting, the metal surfaces disintegrate into fine particles of metals, metal carbides and oxides, etc. Preventing metal dusting in industrial processes is essential to achieve high economic efficiency and has presented a great challenge in materials science community. While intensive research effort has been focused on the performance and development of a wide variety of materials that may resist the carburization and creep, very little is understood about the underlying mechanisms that dictate the dusting processes [6].

Given the fact that both the Boudouard and steam–carbon reactions in the gas-phase are extremely unfavorable energetically, surfaces of stainless steels and alloys must play a key role in catalyzing the reactions. There have been active research efforts to address the dusting processes on surfaces of various stainless

*Corresponding author.

0920-5861/99/$ – see front matter
PII: S0920-5861(98)00492-1

steels and alloys mainly based on phenomenological models. We have recently undertaken a series of studies on dusting at surfaces of various transition metals and their oxides by performing quantum-mechanical first principles calculations [7]. In this article, we report the results on dusting at transition metal oxide surfaces via the Boudouard reaction. The results on dusting reactions on transition metal surfaces will be presented elsewhere. Transition metal oxides such as FeO and NiO are commonly present on surfaces of stainless steels and alloys used in synthesis gas production.

Many practical observations suggest that the oxide contents in the stainless steels or alloys significantly minimize dusting, but the fundamental reasons remain unknown [8,9]. Understanding the dusting mechanisms at the metal oxide surfaces is certainly an essential step towards understanding the dusting phenomena on materials used in practical processes. We show in this work that quantum-mechanical calculations are capable of unraveling some of the detailed fundamental processes taking place in metal dusting. We hope this knowledge will lead to a useful guidance on materials selection to achieve optimal dusting resistance.

The present study focuses mainly on the Boudouard reaction at FeO(1 0 0) surface [3–5]. The system is chosen because the reaction provides elemental carbon for the dusting reaction and FeO is an essential component of stainless steel surfaces. Our calculations utilize ab initio density functional theory (DFT) under both local spin density (LSD) and gradient corrected non-local spin density (NLSD) approximations [10]. DFT has been widely used in electronic structure calculations for molecular systems containing transition metals and has proven particularly efficient to deal with molecular interactions where electronic correlation effect is important. In Section 2, we describe the computational details. The cluster models used to describe the dusting systems are presented in Section 3. The calculated results and discussions will be presented in Section 4. One of the important goals of this study is to elucidate why transition metal oxides are capable of resisting dusting attack. This is accomplished by examining the energetics of the dusting processes. Finally, Section 5 will summarize the conclusions that may be derived from this study.

2. Computational details

Our DFT calculations utilize the double-numerical basis functions augmented with polarization functions provided by the DMol package [11]. The spin polarized computational scheme is adopted to optimize the total electronic energy. The LSD calculation employs the Vosko–Wilk–Nusair local correlation functional [12] and the NLSD calculations utilize the Becke's gradient-corrected exchange and Perdew–Wang's gradient-corrected correlation functionals with the total energy calculated in an iterative manner [13,14]. The Kohn–Sham equation is solved using fine grids. Due to the open-shell nature arising from the large number of unpaired d-electrons in the Fe-atoms, DFT calculations for systems containing transition metals are often computationally challenging. To facilitate the SCF convergence, we utilize a charge smearing function to populate a small fractional electron to the low lying virtual orbitals and then removed the charge self-consistently until the total energy becomes steady and spin contamination essentially vanishes. The core electrons (1s for C and O and 1s2s2p for Fe) are frozen to simplify the computation. Numerical tests suggest that the frozen scheme does not significantly change the structure and energetics.

For CO and C adsorption, we perform geometry optimization at NLSD level with a fixed cluster structure of FeO(1 0 0). To simplify the computation, in all the other cases, geometry optimization is carried out only at the LSD level for evaluation of dusting energetics; single point energy calculations at NLSD level are then performed using the optimized LSD geometries to obtain better energetics while still maintaining good structural accuracy. Effect of lattice relaxation upon dusting is investigated by examining CO adsorption on clusters using a carefully selected optimization scheme.

3. Cluster models

We employ cluster models of the FeO(1 0 0) surface to simulate the CO adsorption and its subsequent reaction with CO and H_2 in the gas phase to form carbon deposited at the surface and gaseous CO_2 and H_2O. The clusters are made from the crystal structure of FeO. Many studies have shown that carefully

selected surface clusters are capable of modeling molecular adsorption phenomena on surfaces [15–17]. In choosing appropriate clusters for theoretical calculations, several important concerns are taken into account. First, the adsorption binding energies of the gas species must be approximately invariant as the cluster size increases. To model bimolecular reactions on surfaces, the clusters usually must be large enough to accommodate all the reaction species without introducing artifacts in the calculations. This frequently imposes great computational difficulties. Since for the Boudouard reaction on metal oxide surfaces, the adsorbed CO interacts mostly with gas phase CO, we only need to examine the cluster sizes based on CO adsorption binding energies. The interaction between any adjacent adsorbates is neglected since it is likely the secondary effect on overall energetics. Second, lattice relaxation upon CO adsorption and dissociation can be an important factor on metal dusting and thus should be considered in the calculations of adsorption structure and energetics. To avoid artifacts, large surface clusters must be used and geometry optimization schemes need to be carefully chosen. Finally, to increase the computational efficiency, the chosen clusters need to be made as symmetric as possible to take advantage of the point-group symmetry in the calculations.

We first examine the effect of cluster size on the CO adsorption binding energy by optimizing the adsorption structure of CO on various sizes of clusters of FeO(1 0 0) surface. Several studies showed that CO adsorbs preferably at the 'on-top' position of metal atoms in transition metal oxides with the carbon atom towards the surfaces [18,19]. Our optimized adsorption geometry, in which CO is adsorbed atop on the center Fe-atom, is indeed in agreement with the result. Fig. 1 displays two clusters of different sizes on which CO is adsorbed. In both cases, the structures of the chosen cluster models with and without CO adsorption exhibit a C_{4v}-symmetry. The adsorption structures were optimized with fixed lattice geometries. The calculated binding energies and the structural parameters of CO adsorption on these clusters are shown in Table 1. While the adsorption structures optimized at both LSD and NLSD levels are in good agreement with each other, the over-binding of the LSD calculation is largely corrected in the NLSD calculation, as expected. The calculated adsorption binding energies on both clusters are approximately the same, suggesting that the surface effect on adsorption is highly localized around the adsorption site, as expected for a solid with highly covalent bonds like FeO. Therefore, structure (a) in Fig. 1 is appropriate to serve as a surface model since it is relatively small and thus computationally easy to handle. The subsequent reaction of the adsorbate with the gas-phase CO is not

Table 1
The calculated NLSD CO adsorption binding energy ΔE on clusters (shown in Fig. 1) and the main optimized bond parameters

Structure	ΔE (kcal/mol)	C–O (Å)	C–Fe (Å)
(a)	−7.815	1.169	1.787
(b)	−7.963	1.172	1.794

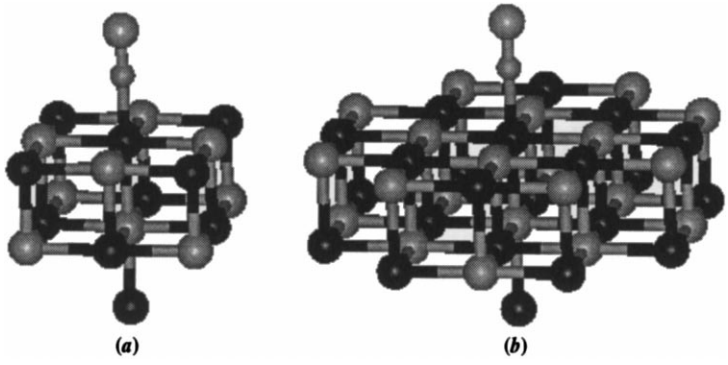

Fig. 1. Cluster models of FeO(1 0 0) surface. The geometry optimization was done at the NLSD level. Here CO is adsorbed atop on an Fe atom.

expected to be affected significantly by the relatively small size of the cluster in view of the large distances between the gaseous species and the surface.

It is understood that the surface atoms will respond to the chemisorption and surface reaction with spontaneous structural reorganization. In particular, structure relaxation of the top-layer atoms near the adsorption sites is expected to occur more significantly upon CO adsorption and dissociation. To investigate the lattice relaxation effect on dusting, we used a 43-atom FeO cluster and optimized both the cluster structure and the cluster with an adsorbed CO on top of the central Fe-atom in three different optimization schemes, as illustrated in Fig. 2. The first scheme is to optimize only the adsorbate with all the surface atoms frozen. The second one is to optimize the adsorbate and all the surface atoms except the atoms at edges and corners, and the third one extends the optimization to eight additional corner atoms. The main optimized adsorption geometric parameters and binding energies are shown in Table 2 (detailed geometric parameters are available upon request). It is seen from Fig. 2 that optimizations involving corner and edge atoms significantly distort the lattice struc-

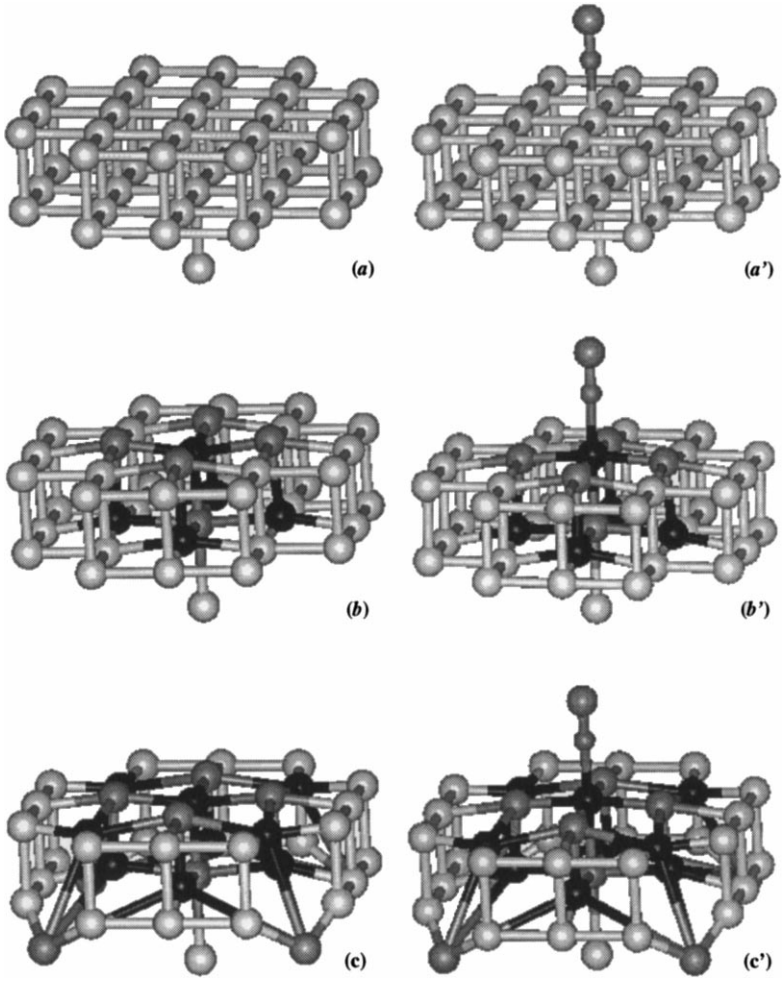

Fig. 2. Clusters used for lattice relaxation. The geometry optimization was done at the NLSD level: (a) optimization only on the adsorbate; (b) optimization on the adsorbate and on the surface atoms highlighted by the gray (O-atoms) and black (Fe-atoms) colors. The white balls represent the surface atoms frozen in their crystal positions; (c) further optimization including the eight atoms at the corners.

Table 2
The calculated CO adsorption binding energy ΔE on clusters shown in Fig. 2 and the main optimized bond parameters. The optimization was done at the NLSD level

Structure	ΔE(kcal/mol)	C–O (Å)	C–Fe (Å)
(a)	−7.963	1.172	1.794
(b)	−11.407	1.180	1.784
(c)	−13.832	1.175	1.776

ture, which will inevitably result in artifact in calculations. This is further evidenced by the much larger CO adsorption binding energy on the relaxed structure. The second optimization scheme also yields considerable perturbation on the lattice atoms around their positions in crystal structure with O-atoms moving slightly out of the surface plane and Fe-atoms being slightly imbedded in the surface. However, each of the atoms being optimized is fully surrounded by neighboring atoms and thus the cluster will not be significantly distorted. Upon CO adsorption, the central Fe-atom moves up slightly towards the adsorbate, as expected. The CO adsorption binding energy on the partially optimized cluster is only about 2 kcal/mol higher than that on the rigid cluster. We thus conclude that the lattice relaxation is not a significant process for dusting at transition metal oxide surfaces. Therefore, in the rest of the paper, we will use only the structure (a) in Fig. 1 to represent the FeO(1 0 0) surface for CO adsorption and dissociation on top of the Fe-atom under the rigid lattice approximation.

It has been suggested that CO may extract an O-atom from TiO_2 surfaces to form CO_2 [20]. We performed geometry optimization for CO to react with the O-atom on an FeO(1 0 0) cluster. The optimized cluster and CO adsorption geometries are shown in Fig. 3. The calculated energy required to extract the O-atom from the FeO(1 0 0) surface is 22.4 kcal/mol at LSD level. The extraction energy is expected to be even higher at NLSD level. Therefore, this is an energetically unfavorable process, although it is interesting to see that the CO_2 is indeed formed. The extraction of an O-atom from the surface creates a large hollow; the adjacent Fe-atoms move further away from the extracting center to form stronger bonding with the neighboring O-atoms instead of forming a closed-packed Fe cluster imbedded on the surface. Therefore, we conclude that CO does not directly interact with the O-atoms on the FeO(1 0 0) surface.

4. Boudouard reaction on FeO(1 0 0)

It is seen from the above that the CO adsorption on the clusters of FeO(1 0 0) surface is very weak. In particular, the CO bond is actually strengthened by interacting with the surface through donation of 5σ electron of CO to the d-band of the surface as evidenced by the shorter CO-bond distance. Furthermore, the atop site of FeO(1 0 0) is the only adsorption mode for CO and thus it is highly unlikely that CO would be dissociatively adsorbed on FeO(1 0 0). It is energeti-

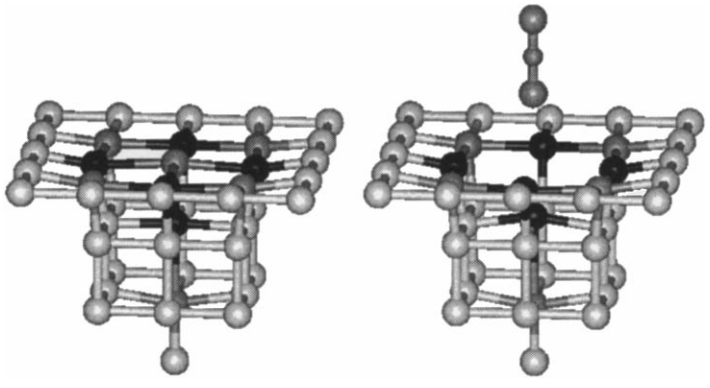

Fig. 3. The cluster model used represents the abstraction process by CO. Geometry optimization was done at both the LSD and NLSD levels. The atoms highlighted in the same fashion as in Fig. 2 are included in the geometry optimization.

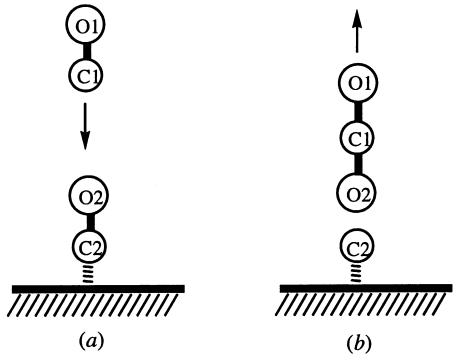

Fig. 4. Schematic scheme representing the reaction path calculations for the Boudouard reaction for normal incidence.

cally difficult for CO to dissociate via reaction between two physisorbed surface species. Therefore, we consider that the Boudouard reaction occurs only between an adsorbed species and a gaseous CO.

We first consider the dusting attack on the adsorbate by CO from the surface normal. This allows us to impose a C_{4v}-symmetry in the calculation. The gas-phase species approach the adsorbate forming CO_2 and leaving the surface with C deposited on the Fe-atom. To describe this process, we performed minimum-energy path calculations to follow the reaction trajectories. This was done by a procedure schematically shown in Fig. 4. Specifically, for the Boudouard reaction, the gas-phase CO first attacks the adsorbate with the C-atom head-on towards the surface (forward reaction); it picks up the O-atom from the adsorbate and bounces back to the gas-phase (backward reaction). In the forward reaction, the distance between the gas-phase C-atom and the surface plane serves as the reaction coordinate, while in the backward reaction the bond length of the adsorbate serves as the reaction coordinate. All other degrees of freedom of the molecular species are optimized under the imposed C_{4V}-symmetry and the rigid lattice approximation.

Fig. 5 displays the calculated energy profile along the minimum-energy path of normal incidence for the Boudouard reaction. Geometry optimization was done only at the LSD level. The NLSD energy was calculated using the geometries obtained in the LSD calculations. In essence, the LSD and NLSD results are in agreement with each other. The calculation suggests that the reaction thermo chemistry at the FeO(1 0 0) surface is energetically unfavorable. In particular, the activation barrier is exceedingly high. Qualitatively, this conclusion is consistent with the observation that the metal oxide surfaces tend to block-dusting [8,9]. The calculation has unraveled the fundamental reason behind this phenomenon.

Fig. 6 displays the collected bond parameter changes along the reaction coordinate. Fig. 6(a) shows the distance of the C-atom of the gas-phase CO from

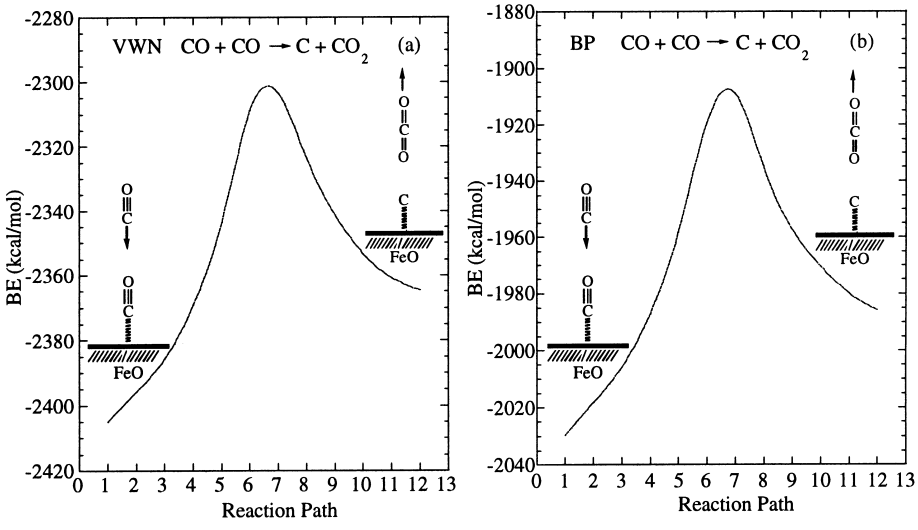

Fig. 5. Energy profiles along the reaction coordinate of the Boudouard reaction calculated at (a) LSD and (b) NLSD levels, respectively.

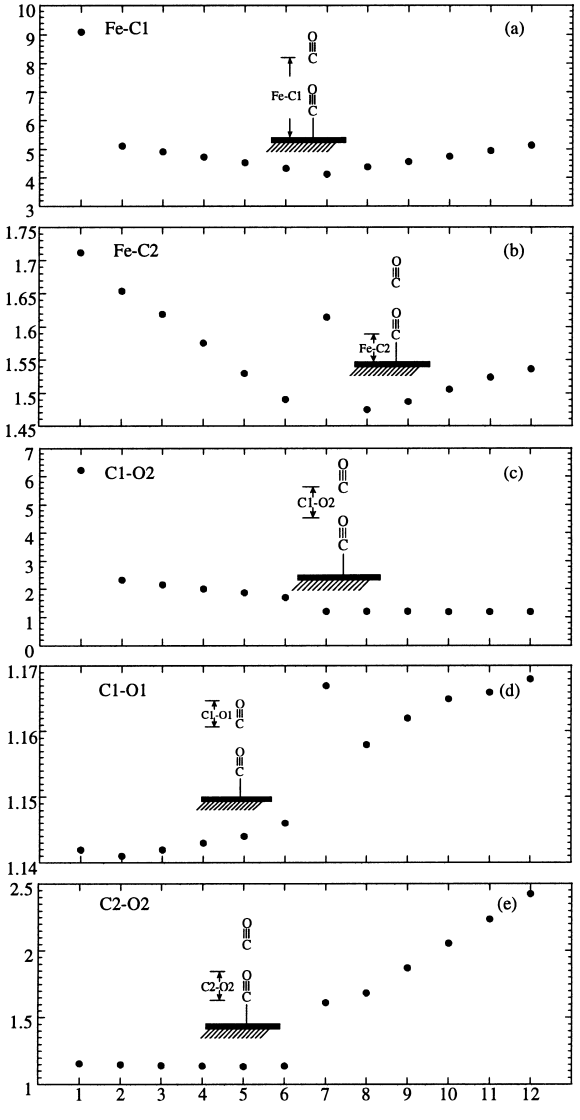

Fig. 6. Structural changes along the reaction path for normal incidence: (a) the distance between the C-atom of the gas-phase CO and the surface; (b) bond-distance between the C-atom of the adsorbed CO and the surface; (c) the distance between the C-atom of the gas-phase CO and the O-atom of the adsorbed CO; (d) C–O bond distance of the gas-phase CO; (e) C–O bond distance of the adsorbed CO.

the surface. As the bond distance reaches 4.12 Å, the gas-phase CO arrives at the transition state. It then picks the O-atom from the adsorbate to form CO_2, which subsequently goes back to the gas phase. Fig. 6(b) depicts the bond distance between the C-atom of the adsorbate and the Fe-atom on which CO is adsorbed. The adsorbate is compressed by the incoming CO towards the surface until the reaction arrives at the transition state at which it bounces back. As CO_2 leaves the surface, the deposited C-atom slightly stretches its bond with the surface and reaches the optimal bond-distance. The change in the bond-distance between the gas phase C-atom and the O-atom of the adsorbate is shown in Fig. 6(c). The two atoms gradually form a double bond, which remains steady after the transition-state. On the other hand, the bond length of the gas-phase CO stretches from the triple-bond distance to the double-bond one, as shown in Fig. 6(d). Finally, the bond-length of the adsorbate is elongated and eventually dissociated along the minimum-energy path (Fig. 6(e)).

Fig. 6 displays the collected bond-parameter changes along the reaction coordinate. Fig. 6(a) shows the distance of the C-atom of the gas-phase CO from the surface. As the bond distance reaches 4.12 Å, the gas-phase CO arrives at the transition state. It then picks the O-atom from the adsorbate to form CO_2 which subsequently goes back to the gas phase. Fig. 6(b) depicts the bond distance between the C-atom of the adsorbate and the Fe-atom on which CO is adsorbed. The adsorbate is compressed by the incoming CO towards the surface until the reaction arrives at the transition state at which it bounces back. As CO_2 leaves the surface, the deposited C-atom slightly stretches its bond with the surface and reaches the optimal bond-distance. The change of the bond distance between the gas phase C-atom and the O-atom of the adsorbate is shown in Fig. 6(c). The two atoms gradually form a double bond, which remains steady after the transition state. On the other hand, the bond-length of the gas-phase CO stretches from the triple-bond distance to the double-bond one, as shown in Fig. 6(d). Finally the bond-length of the adsorbate is elongated and eventually dissociated along the minimum-energy path (Fig. 6(e)).

It is important to examine the charge-transfer processes in the gas-surface interface along the reaction pathway in order to fully understand why metal oxides are dusting resistant. In Fig. 7, we show the calculated Mulliken gross charges and the individual atomic charges of the reaction species. It is seen from Fig. 7(a) that the gross charges of the reaction species in the entire reaction process are positive. These

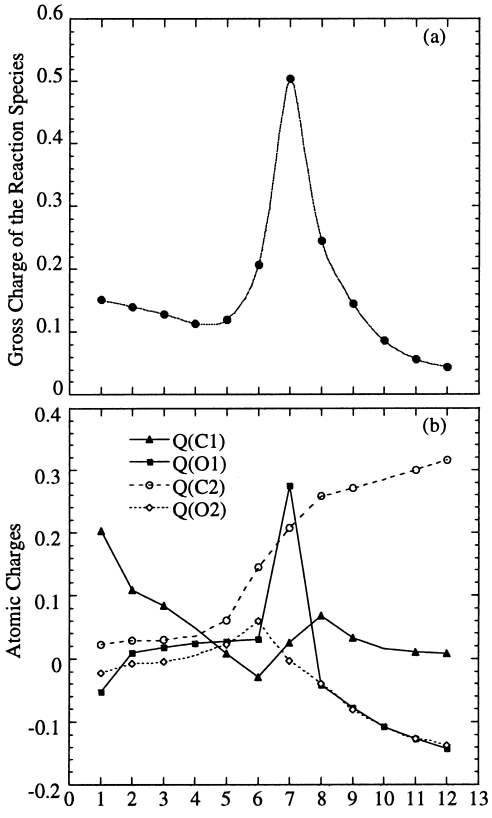

Fig. 7. Mulliken population distribution along the reaction coordinate: (a) the gross charge of the reaction species and (b) atomic charges of the reaction species. Here C1 and O1 are for the C- and O- atoms of the gas-phase CO and C2 and O2 for the C- and O-atoms of the adsorbed CO.

charges represent the amount of overall charge transferred to the surface. The charge transfer increases near the transition state and rapidly diminishes with the formation of CO_2. The gross charge variation of the reaction species can be further analyzed in detail by examining the individual atomic charges of the reaction species, as shown in Fig. 7(b). First, the charge of the C-atom of the adsorbate (C2) increases monotonically along the reaction path. This is because the dissociation of the adsorbate results in a much stronger bonding between the C-atom and the surface (the calculated NLSD bonding energy of C on the surface is −82.22 kcal/mol). As a consequence, electron donation from the adatom to the surface increases. Second, the small negative charges on the two O-atoms of the reaction species are mainly due to the triple-bond nature of CO and they converge to the same value as CO_2 is formed as expected. The maximum charge transfer to the surface observed in Fig. 7(a) is the overall consequence of stronger bonding of adatom-surface and the electron withdrawing effect from the gas-phase O-atom to the surface bridged by the O-atom of the adsorbate, as seen in Fig. 7(b). The population analysis suggests that the O-atoms in the oxides prompt the metals in a relatively higher oxidation states and thus reduce the tendency of electron back donation. This is in fact consistent with the relatively small CO adsorption energy. As a consequence, the C–O bond becomes strengthened, which prevents Boudouard reaction from occurring.

Our calculation suggests that all the electronic states near the Fermi level are contributed mostly by the surface states, which are primarily composed of the d-orbitals of the Fe atoms and the p-orbitals of the surface O-atoms. The bonding states resulting from the orbital interaction between the adsorbate and the surface lie a few electron volts below the Fermi level. In particular, the interaction between the 5σ-orbital of CO, which is known to be slightly anti-bonding [16], and the 4s and $3d_{z^2}$ orbitals of the adsorbing Fe-atom give rise to the adsorbate–surface bonding with electron donation from CO to the surface in nature, which would strengthen the C–O bond of the adsorbate. On the other hand, the orbital interaction between the 2π-orbital of CO and the d_{xz} and d_{yz} orbitals of the Fe-atom results in electron back donation from the surface to the adsorbate. Since the 2π-orbital of CO is anti-bonding, the back donation would cause weakening of the C–O bond. Furthermore, the strong covalent Fe–O bonds of the FeO surface tend to remove the d-electrons from the Fe-atoms towards the O-atoms. Consequently, the electron back donation is limited. Indeed, the calculated gross charges of the reaction species indicate that the electron donation prevails over the back donation in the present case, and as a result, the C–O bond of the adsorbate is very strong. This explains successfully why C–O dissociation is difficult at the FeO surface.

5. Summary

In this article, we have used density functional theory to investigate the possible cause of one of

the major metal dusting processes represented by the Boudouard reaction at FeO(1 0 0) surface. The calculated minimum-energy path indicates that the reaction is extremely unfavorable both thermochemically and kinetically. The population analysis along the reaction path provides detailed insight into the charge transfer processes in the gas–surface interface. The calculated electronic states and the population distribution suggest that the CO adsorption at FeO(1 0 0) surface is dictated by the electron donation of the 5σ-orbital of CO to the 4s and $3d_{z^2}$ orbitals of Fe and the small back donation from the d_{xz} and d_{yz} orbitals of Fe to the 2π-orbital of CO. The calculations suggest that metal oxides are not catalytic accelerators for the Boudouard reaction leading to metal dusting, thereby reducing the amount of carbon produced by the Boudouard reaction on a given surface.

Although the present work dealt with the dusting phenomena only at the FeO(1 0 0) surface, the basic conclusions derived from this work may also be applicable to other transition metal oxide surfaces. In fact, we have undertaken similar studies on NiO surfaces and concluded that both the Boudouard and steam–carbon reactions would be difficult due to the unfavorable energetics. This is consistent with the extensive studies in the literature on CO adsorption on surfaces of various metal oxides, such as MgO [21], TiO_2 [22], and ZnO [23]. In all the cases, CO was found to be weakly adsorbed on well-aligned oxide surfaces and chemisorption occurs only at surface defects and vacancies. Indeed, we have found that CO can be readily activated at the defect/vacancy sites with a large adsorption energy and a considerably elongated bond [24], which will ultimately lead to metal dusting. It should be pointed out, however, that the present study mainly focuses only on one CO adsorption configuration, which appears to be the dominant adsorption pattern. Other configurations, while less energetically possible, may also be present in practice. In particular, the 'side-on' adsorption on the surface may lead to much easier bond dissociation and thus facilitate the Boudouard and steam–carbon reactions. We will investigate the effect of various adsorption patterns on these reactions in a future study.

An important conclusion from this work is that in most cases the normal oxides present on stainless steels should prevent Boudouard carbon deposition. However, the presence of defects in these oxides will yield sites for local carbon deposition to occur. Indeed, experimental studies by Yates [19] on CO adsorption on TiO_2 surfaces have shown that CO is adsorbed only at the defect sites. As a result, the dusting attack should take the form of pits occurring at these local sites as carbon diffuses into the metal at these sites, ultimately causing the loss of metal from these sites. The observation of pitting attack as a result of metal dusting has not been adequately explained in the prior literature, but based on this work it is clear that pitting should be the preferred mode of attack. However, this work does not explain the occurrence of crevice attack which is also often observed in metal dusting situations.

References

[1] W.R. Davis, R.J. Dlawson, G.R. Rigby, Nature 171 (1953) 756.
[2] P.L. Walker jr., J.F. Rakszawski, G.R. Imperial, J. Phys. Chem. 63 (1959) 133.
[3] W.B. Hoyt, R.H. Caughey, Corrosion 15 (1959) 21.
[4] J.A. Richardson, Nitrogen 205 (1993) 49.
[5] H.J. Grabke, R. Krajak, E.M. Müller-Lorenz, Werkstoffe und Korrosion 44 (1993) 89.
[6] H.J. Grabke, R. Krajak, J.C. Nava Paz, Corrosion Sci. 35 (1993) 1141.
[7] H. Cheng, D.B. Reiser, P.M. Mathias, S.W. Dean Jr., , AIChE J. 44 (1998) 188.
[8] I. Koszman, in: S.A. Jansson, Z.A. Foroulis (Eds.), High Temperature Gas–Metal Reactions in Mixed Environments, vol. 155, Metallurgical Society of AIME, 1973.
[9] R.H. Kane, in: B.J. Moniz, W.I. Pollock (Eds.), Process Industries Corrosion – The Theory and Practice, vol. 45, National Association of Corrosion Engineers, 1986.
[10] J.K. Labanowski, J.W. Andzelm, Density Functional Methods in Chemistry, Springer, New York, 1991.
[11] DMOL, v2.3.6, Biosym Technologies, San Diego, CA, USA, 1994.
[12] S.J. Vosko, L. Wilk, M. Nusair, Can. J. Phys. 58 (1980) 1200.
[13] A.D. Becke, Int. J. Quan. Chem. 23 (1983) 1916.
[14] J.P. Perdew, Phys. Rev. Lett. 55 (1985) 1665.
[15] P.E.M. Siegbahn, U. Wahlgren, Int. J. Quan. Chem. 42 (1992) 1149.
[16] M.A. van Daelen, Y.S. Li, J.M. Newsam, R.A. van Santen, J. Phys. Chem. 100 (1996) 2279.
[17] C. Mijoule, Y. Bouteiller, D.R. Salahub, Surf. Sci. 253 (1991) 375.
[18] H. Kobayashi, M. Yamaguchi, Surf. Sci. 214 (1989) 466.

[19] J.T. Yates Jr., , Surf. Sci. 299 (1994) 731.
[20] W. Göpel, G. Rocker, Feierabend, Phys. Rev. B 28 (1983) 3427.
[21] K. Jug, G. Geudtner, Quantum chemical study of carbon monoxide adsorption at the MgO(1 0 0) surface, J. Chem. Phys. 105 (1996) 5285.
[22] A. Linsebigler, G. Lu, J.T. Yates, CO chemisorption on TiO_2(1 1 0): oxygen vacancy site influence on CO adsorption, J. Chem. Phys. 103 (1995) 9438.
[23] J.E. Jaffe, A.C. Hess, Ab initio study of a CO monolayer adsorbed on the (1 0 1 0) surface of ZnO, J. Chem. Phys. 104 (1995) 3348.
[24] H. Cheng, D.B. Reiser, S.W. Dean, Jr., in preparation.